

Color-octet effects in radiative Υ decays

Fabio Maltoni*

CERN, TH Division, Geneva, Switzerland

Andrea Petrelli†

Argonne National Laboratory, HEP Division, Argonne, Illinois 60439

(Received 26 June 1998; published 18 February 1999)

We investigate the effects of color-octet contributions to the radiative Υ decay within the Bodwin, Braaten, and Lepage nonrelativistic QCD (NRQCD) framework. We compute the short-distance coefficients at next-to-leading order (NLO) in α_s for the most relevant color-octet intermediate states and consider photons coming both from the coupling to hard processes (“direct”) and by collinear emission from light quarks (“fragmentation”). An estimate for the nonperturbative matrix elements which enter in the final result is then obtained. By comparing the NRQCD prediction at NLO for total decay rates with the experimental data, it is found that the nonperturbative parameters must be smaller than expected from the naive scaling rules of NRQCD. Nevertheless, color-octet contributions to the shape of the photon spectrum turn out to be significant. [S0556-2821(99)02705-8]

PACS number(s): 13.25.Gv, 11.10.St, 12.38.Bx

I. INTRODUCTION

Since the early times of QCD, heavy quarkonia decays have been considered among the most promising processes to test the perturbative sector of the theory and to extract the value of the strong coupling at scales of the order of the heavy-quark mass. In addition to the calculation and comparison of full inclusive decay rates, much attention has been devoted to the decays in which one photon is emitted, and its energy measured [1]. Experimental data on the direct photon spectrum in Υ decays have been compared [2,3], up to now, under the assumption of a factorization between a short-distance part describing the annihilation of the heavy-quark pair in a color-singlet state and a nonperturbative long-distance factor, related to the value of the nonrelativistic wave function at the origin.

Recently Bodwin, Braaten, and Lepage (BBL) [4] provided a new framework to study quarkonium decay within QCD. Introducing an effective nonrelativistic theory (NRQCD), perturbative and gauge-invariant factorization is obtained by including in the decay intermediate $Q\bar{Q}$ states with quantum numbers different from those of the physical quarkonium state. The relative importance of various contributions depends on short-distance coefficients which are calculable by standard perturbative techniques, and on long-distance matrix elements, which can be either extracted phenomenologically from the data or calculated on the lattice. In the end one is able to organize all these terms in a double perturbative series in the strong coupling α_s and in the relative velocity v of the heavy quarks, and then to make predictions at any given order of accuracy.

In quarkonia decays, photons arise from electromagnetic

coupling to both heavy and light quarks. While contributions coming from the former, at leading order (LO) in α_s in the color-singlet model (CSM), i.e., at the lowest order in v expansion in NRQCD, have been known for a long time and are one of the first tests of QCD [2,3], LO contributions coming from collinear emission from light quarks have surprisingly been considered only recently by Catani and Hautmann [5]. The inclusion of these “fragmentation” contributions within the CSM was found to greatly affect the photon spectrum in the Υ decay at low values of the energy fraction taken away by the photon [5]. Moreover, one finds that at LO such a contribution comes entirely from the gluon, as the decay into light quarks vanishes.

It then becomes important to assess to what extent this picture remains unchanged once color-octet contributions are included. The aim of this work is to investigate the effects of such color-octet intermediate states on the photon spectrum, at NLO order in α_s , including the coupling of the photons to light quarks and gluons. In fact, while the order of magnitude of octet contributions is predicted using scaling rules, and found to be suppressed by powers of v with respect to the LO color-singlet ones, their short-distance coefficients receive contributions at lower order of α_s , and are then numerically enhanced. Furthermore, once leading logarithmic corrections are included, it is found that, contrary to the color-singlet case, quark and gluon fragmentation into a photon appears at the same order in the α_s , α_{em} expansion and there is no signature to distinguish between the two.

The paper is organized as follows. In Sec. II we summarize the analysis of quarkonium decay into photons and hadrons in the framework of NRQCD. Section III describes the NLO calculation and the technique used to isolate and cancel or subtract IR and collinear divergences. In Sec. IV we give estimates for the nonperturbative matrix elements by comparing the NLO predictions for total decay rates with experimental data. Finally, we present a numerical study of the impact of octet states on the shape of the photon spectrum. The last section is devoted to our conclusions. Appendix A collects symbols and notation, Appendix B collects the re-

*Permanent address: Dipartimento di Fisica dell’Università and Sez. INFN, Pisa, Italy. Email address: fabio.maltoni@cern.ch

†Email address: petrelli@hep.anl.gov

sults for the Born decay rates in D dimensions. A summary of the NLO results is provided in Appendix C, where differential decay rates are presented in their final form, after cancellation of all singularities.

II. NRQCD AND FRAGMENTATION

A consistent description of the photon energy spectrum in $Y \rightarrow \gamma + X$ decay requires the inclusion of the fragmentation components [5]. The differential photon decay can be expressed in terms of a convolution between partonic kernels C_a and the fragmentation functions $D_{a \rightarrow \gamma}$:

$$\begin{aligned} \frac{d\Gamma}{dz} &= C_\gamma(z) + \sum_{a=q,\bar{q},g} \int_z^1 \frac{dx}{x} C_a(x, \mu_F) D_{a \rightarrow \gamma}\left(\frac{z}{x}, \mu_F\right) \\ &\equiv C_\gamma + \sum_a C_a \otimes D_{a \rightarrow \gamma}, \end{aligned} \quad (1)$$

where $z = E_\gamma/m_Q$ is the rescaled energy of the photon (m_Q is the heavy-quark mass). The first term corresponds to what is usually called the ‘‘prompt’’ or ‘‘direct’’ photon production where the photon is produced directly in the hard interaction while the second one corresponds to the long-distance fragmentation process where one of the partons fragments and transfers a fraction of its momentum to the photon.

Each type of parton a contributes according to the process-independent parton-to-photon fragmentation functions $D_{a \rightarrow \gamma}^B$ and the sum runs over all partons. Note that although the fragmentation functions are nonperturbative, we can assign a power of coupling constants, based on naively counting the couplings necessary to radiate a photon: since the photon couples directly to the quark, $D_{q \rightarrow \gamma}$ is of $\mathcal{O}(\alpha_{\text{em}})$, while we might expect that $D_{g \rightarrow \gamma}$ is of $\mathcal{O}(\alpha_{\text{em}}\alpha_s)$. An explicit calculation at leading order in α_s gives

$$z D_{q \rightarrow \gamma}(z) = e_q^2 \frac{\alpha_{\text{em}}}{2\pi} z \mathcal{P}_{q \rightarrow \gamma}(z) \log \frac{Q^2}{\Lambda^2}, \quad (2)$$

$$z D_{g \rightarrow \gamma}(z) = 0, \quad (3)$$

where the $\log(Q^2/\Lambda^2)$ in Eq. (2) comes from the integration over the transverse momentum of the emitted photon and Λ is a collinear cut-off that reveals the breaking of the perturbative approach and can be chosen of the order of Λ_{QCD} . The photon fragmentation functions evolve with Q^2 just as the usual hadronic fragmentation functions do, as a result of gluon bremsstrahlung and $q\bar{q}$ pair production. Such evolution can be derived from a set of coupled equations, which are the usual Altarelli-Parisi equations but with an added term that takes into account the leading behavior in Eq. (2). The main result of the evolution is that $D_{g \rightarrow \gamma}$ acquires a nonvanishing contribution so that all the $D_{a \rightarrow \gamma}$ show the typical logarithmic growth of Eq. (2). This leads to using the following leading-log approximation (LLA) for the fragmentation functions [6]:

$$D_{a \rightarrow \gamma}(z, Q) = \frac{1}{b_0} \frac{\alpha_{\text{em}}}{\alpha_s(Q)} f_a(z), \quad (4)$$

where $f_a(z)$ are to be extracted from the data. This shows explicitly that in general the determination of the spectrum at $\mathcal{O}(\alpha_{\text{em}}\alpha_s^k)$ requires the knowledge of partonic kernels C_a in Eq. (1) at $\mathcal{O}(\alpha_s^{k+1})$. This observation was first made, in quarkonia decays, by Catani and Hautmann [5] who evaluated the effects of fragmentation contributions to the photon energy spectrum within the CSM. They found a strong enhancement in the region of small z , where soft radiation becomes dominant.

In the NRQCD perspective, a heavy-quarkonium state is represented by a superposition of infinite $Q\bar{Q}$ pair configurations organized in powers of v ; $v \equiv \langle v^2 \rangle^{1/2}$ is the average velocity of the heavy quark in the quarkonium rest frame. Within this framework, the decay width is expanded in terms of the matrix elements of four-fermion operators (that create and annihilate a given $Q\bar{Q}$ pair) times perturbative coefficients associated to each operator. By implementing the NRQCD factorization formalism within the fragmentation picture, the effects of higher Fock components in the quarkonium state can therefore be evaluated systematically.

The NRQCD expansion for the coefficients $C_i(x)$ reads

$$C_i = \sum_{\mathcal{Q}} C_i[\mathcal{Q}], \quad i = \gamma, q, \bar{q}, g, \quad (5)$$

$$C_i[\mathcal{Q}] = \hat{C}_i[\mathcal{Q}][(\alpha_s(m_Q), \mu_\Lambda)] \frac{\langle Y | \mathcal{O}(\mathcal{Q}, \mu_\Lambda) | Y \rangle}{m^{\delta_{\mathcal{Q}}}}, \quad (6)$$

where μ_Λ is the NRQCD factorization scale and $\hat{C}_i[\mathcal{Q}](x, \alpha_s(m_Q), \mu_\Lambda)$ the perturbative coefficients (here we have dropped the dependence of \hat{C}_i on the fragmentation scale μ_F). The NRQCD sum is performed over all the relevant spin, angular momentum and colour configurations \mathcal{Q} that contribute at a given order in v . In the case of a Y , the structure of the Fock state at order v^4 is

$$\begin{aligned} |Y\rangle &= \mathcal{O}(1) |b\bar{b}[^3S_1^{[1]}]\rangle + \sum_J \mathcal{O}(v) |b\bar{b}[^3P_J^{[8]}]\rangle \\ &+ \mathcal{O}(v^2) |b\bar{b}[^1S_0^{[8]}]\rangle + \mathcal{O}(v^2) |b\bar{b}[^3S_1^{[1,8]}]\rangle. \end{aligned} \quad (7)$$

As a consequence, Eq. (5) can be written in the following explicit form:

$$\begin{aligned} C_i &= \hat{C}_i[^3S_1^{[1]}] \frac{\langle Y | \mathcal{O}_1(^3S_1) | Y \rangle}{m^2} + \hat{C}_i'^{[3S_1^{[1]}]} \frac{\langle Y | \mathcal{P}_1(^3S_1) | Y \rangle}{m^4} \\ &+ \sum_J \hat{C}_i[^3P_J^{[8]}] \frac{\langle Y | \mathcal{O}_8(^3P_J) | Y \rangle}{m^4} \\ &+ \hat{C}_i[^1S_0^{[8]}] \frac{\langle Y | \mathcal{O}_8(^1S_0) | Y \rangle}{m^2} \\ &+ \hat{C}_i[^3S_1^{[8]}] \frac{\langle Y | \mathcal{O}_8(^3S_1) | Y \rangle}{m^2} + \mathcal{O}(v^6). \end{aligned} \quad (8)$$

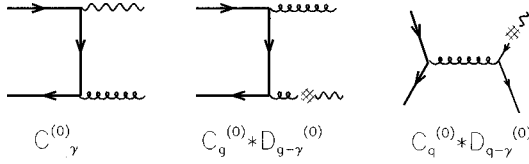


FIG. 1. Sample of LO Feynman diagrams: direct and fragmentation.

Let us consider the direct contributions ($i = \gamma$). The leading color-singlet dimension-six operator contribution is of $O(\alpha_s^2 \alpha_{\text{em}})$, and the \mathcal{P}_1 -operator contribution is suppressed by v^2 . All the color-octet processes start contributing at $O(\alpha_s \alpha_{\text{em}} v^4)$. By naive power counting, and using the approximate relation $\alpha_s \sim v^2$, one finds therefore that the octet states contribute to the same order as the singlet relativistic corrections and might be comparable in size to these. Moreover differential quantities are obviously sensitive to the details of the kinematics and so it may happen that contributions that are suppressed by standard counting rules are actually leading, in some particular region of the phase space.

LO diagrams are shown in Fig. 1. By considering the following perturbative QCD expansions of the coefficients $C_a[\mathcal{Q}]$ and of the fragmentation functions $D_{i \rightarrow j}$:

$$\begin{aligned} C_a[\mathcal{Q}] &= (\hat{C}_a^{(0)}[\mathcal{Q}] + \hat{C}_a^{(1)}[\mathcal{Q}]) \frac{\langle Y | \mathcal{O}(\mathcal{Q}) | Y \rangle}{m^{\delta_{\mathcal{Q}}}} \\ &\equiv C_a^{(0)}[\mathcal{Q}] + C_a^{(1)}[\mathcal{Q}] + \dots, \end{aligned} \quad (9)$$

$$D_{i \rightarrow j} = D_{i \rightarrow j}^{(0)} + D_{i \rightarrow j}^{(1)} + \dots, \quad (10)$$

one is able to write the general structure of the LO spectrum,

$$\begin{aligned} \frac{d\Gamma^{(0)}}{dz} &= \sum_{\mathcal{Q}} \{ C_\gamma^{(0)}[\mathcal{Q}] + C_g^{(0)}[\mathcal{Q}] \otimes D_{g \rightarrow \gamma}^{(0)} \\ &\quad + 2C_q^{(0)}[\mathcal{Q}] \otimes D_{q \rightarrow \gamma}^{(0)} \}. \end{aligned} \quad (11)$$

Since the LO color-octet contributions have a two particle final state, the kinematics is fixed and the delta function $\delta(1-x)$ of the short-distance coefficient transforms the convolutions in trivial products

$$\begin{aligned} \frac{d\Gamma^{(0)}}{dz} &= \sum_{\mathcal{Q}} [\Gamma_{\text{Bom}}(\mathcal{Q} \rightarrow g\gamma) \delta(1-z) \\ &\quad + 2\Gamma_{\text{Bom}}(\mathcal{Q} \rightarrow gg) D_{g \rightarrow \gamma}^{(0)}(z)] \\ &\quad + 2 \sum_q \Gamma_{\text{Bom}}({}^3S_1^{[8]} \rightarrow q\bar{q}) D_{q \rightarrow \gamma}^{(0)}(z), \end{aligned} \quad (12)$$

where the first sum is performed over the lowest-order non-zero octet configurations $\mathcal{Q} = {}^1S_0^{[8]}, {}^3P_0^{[8]}, {}^3P_2^{[8]}$, while the second one over the flavors of the light quarks. As Eq. (12) shows, at leading order the color-octet contributions are pro-

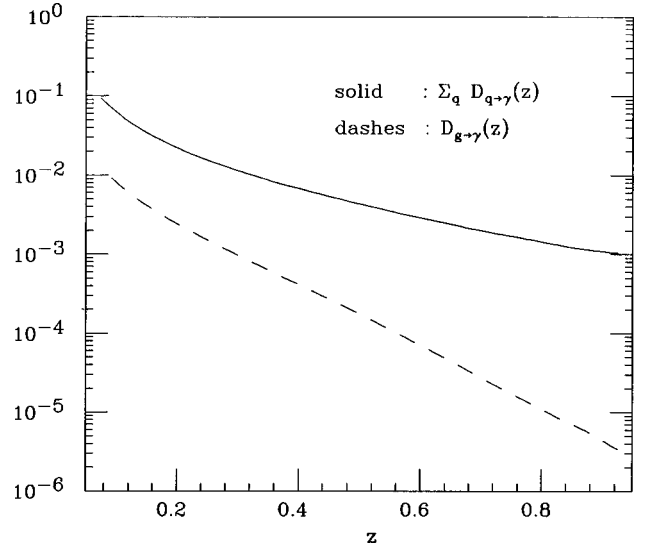


FIG. 2. Fragmentation functions of a light parton into a photon according to Ref. [8].

portional to the fragmentation functions and to terms proportional to $\delta(1-z)$ which do not contribute¹ for $z < 1$.

The fragmentation functions of a light parton into a photon have been calculated and modeled by several groups [8,9]. We have to stress that while at high values of Q^2 , $D_{a \rightarrow \gamma}(x, Q)$ are fully calculable in perturbative QCD, for lower values nonperturbative and beyond leading logarithm corrections are sizeable. In particular, the nonperturbative part of the fragmentation functions becomes model dependent. In this paper we employ the set recently developed by Bourhis, Fontannaz, and Guillet [8], where nonperturbative effects are obtained by means of the vector meson dominance model. At the scales relevant in our case, these effects dominate and indeed affect our predictions for the photon spectrum mainly for low values of z . With respect to this, we may have to consider our results in this area of the phase space, rather uncertain. Nevertheless the heart of our conclusions rely on the relative importance of the quark-to-photon respect to the gluon-to-photon fragmentation function. This fact can be approximately considered model independent [see, e.g., Ref. [8] where different parametrizations are compared and Fig. 2 where functions $D_{g \rightarrow \gamma}(z)$ and $\sum_q D_{q \rightarrow \gamma}(z)$ are shown]. Moreover it will be clear from the results presented in the following section that at low values of z the LO picture remains unchanged (the process of a gluon into a photon is dominant in color-octet C -even states decay while the fragmentation from quark into a photon is the leading process in the case of a ${}^3S_1^{[8]}$ state) and so one can trace back the effects of a different set of fragmentation functions by comparing it with the one shown in Fig. 2.

¹Although we did not include these ‘‘direct’’ terms in our analysis, we expect that resummation of higher order effects for $z \sim 1$ will induce an effective smearing of the delta function and ‘‘feed down’’ some photons to lower values of z [7]. This point will be discussed in more detail in the sequel.

III. NLO RADIATIVE DECAYS: THE CALCULATION TECHNIQUE

In this section we briefly describe the strategy for the calculation of higher-order corrections. A consistent calculation of these entails the evaluation of the real and virtual emission diagrams, carried out in D dimensions. The UV divergences present in the virtual diagrams are removed by the standard renormalization. The IR divergences appearing after the integration over the phase space of the emitted parton are cancelled by similar divergences present in the virtual corrections, or by higher-order corrections to the long-distance matrix elements [4]. Collinear divergences, finally, are either cancelled by similar divergences in the virtual corrections or by factorization into the NLO fragmentation functions. The evaluation of the real emission matrix elements in D dimensions being particularly complex, we follow in this paper the technique developed in Ref. [10] and already employed in Refs. [11,12], whereby the structure of soft and collinear singularities in D dimensions is extracted by using universal factorization properties of the amplitudes. Thanks to these factorization properties, the residues of all IR and collinear poles in D dimensions can be obtained without an explicit calculation of the full D -dimensional real matrix elements. In general they only require the knowledge of the D -dimensional Born-level amplitudes, a much simpler task. The isolation of these residues allows the complete cancellations of the relative poles in D dimensions to be carried out, leaving residual finite expressions, which can then be evaluated exactly directly in $D=4$ dimensions. In this way one can avoid the calculation of the full D -dimensional real-emission matrix elements. Furthermore, the four-dimensional real matrix elements that will be required have been known in the literature for quite some time [13,14]. The study of the soft behavior of the real-emission amplitudes was already presented in Refs. [11,12] and we made substantial use of those results.

To be more specific, let us consider the three-body decay processes $Q^{[1,8]} \rightarrow k_1 + k_2 + k_3$, where $Q^{[1,8]} \equiv Q\bar{Q}^{[2S+1]L_J^{[1,8]}}$. Using the conservation of energy-momentum and rotational invariance, it is straightforward to verify that there are only two independent variables, which we chose to be x_i , the fraction of energy of the parton whose spectrum we are interested in, and y , the cosine of the angle of such parton with one of the other two. Within this choice, the differential decay width in D dimensions reads

$$\begin{aligned} C_i^{(1)}[Q] &= \frac{\Phi_{(2)}}{2M} \frac{N}{K} \frac{1}{S_1} x_i^{1-2\epsilon} (1-x_i)^{-1-\epsilon} \\ &\quad \times \int_0^1 dy [y(1-y)]^{-1-\epsilon} f_R[Q](x_i, y) \\ &\quad + \frac{\Phi_{(2)}}{2MS_2} f_V[Q] \delta(1-x_i) \\ &\equiv C_i^{(R)}[Q] + C_i^{(V)}[Q]. \end{aligned} \quad (13)$$

The NLO spectrum coefficients are the sum of the virtual and the real (R) and the virtual (V) QCD corrections. In

general both channels ggg and $q\bar{q}g$ contribute to the real term, the $S_{1,2}$ are factors that account for the right counting for identical particles in the final state, and for the multiplicity of the various corrections, and $\Phi_{(2)}$ is the total two-body phase space in D dimensions:

$$\Phi_{(2)} = \frac{1}{8\pi} \left(\frac{4\pi}{M^2} \right)^\epsilon \frac{\Gamma(1-\epsilon)}{\Gamma(2-2\epsilon)}, \quad (14)$$

while N and K are defined as

$$\begin{aligned} N &= \frac{M^2}{(4\pi)^2} \left(\frac{4\pi}{M^2} \right)^\epsilon \Gamma(1+\epsilon), \\ K &= \Gamma(1+\epsilon)\Gamma(1-\epsilon) \sim 1 + \epsilon^2 \frac{\pi^2}{6}. \end{aligned} \quad (15)$$

The function $f(x, y)$ is defined as

$$f_R[Q](x_i, y) = (1-x_i)y(1-y) \overline{\sum} |A_R[Q](x_i, y)|^2 \quad (16)$$

$$f_V[Q] = 2 \operatorname{Re} \overline{\sum} (A_B A_V^*). \quad (17)$$

Since divergences can appear only at the border of phase space, i.e., $y=0$, $y=1$, $x_i=0$, $x_i=1$, f_R is finite for all values of x and y within the integration domain. Therefore all singularities of the total decay rates can be easily extracted by isolating the $\epsilon \rightarrow 0$ poles from those factors in Eq. (13) that explicitly depend on x_i and y . It must be noted that an infrared divergence arises in the limit $x_i \rightarrow 0$ when $i=g$, giving a term of the form $\sim \log x_g$ in the width. Nevertheless we are not interested in regularizing such a divergence, since, in this case, the physical resolution of the detector works as a physical cutoff. For the same reason the virtual gluon emission at $x_g=0$ has not been included in the account of the multiplicities.

The virtual coefficients can be extracted straightforwardly from Ref. [12]. The calculation of the real coefficients is much more complicated, and it has been carried out by exploiting the soft properties of the amplitude obtained in Refs. [11,12]. To illustrate the fundamental steps of the calculation of the real part, we consider here the $C_g^{(R)}[Q]$ coefficients, with Q being one among the C -even configurations $^1S_0^{[8]}$, $^3P_0^{[8]}$, $^3P_2^{[8]}$. Let also $n_f=0$ for the time being, so that we neglect contributions coming from the decay into $q\bar{q}g$. In this case we reorganize the first term of Eq. (17) by expanding the structure in powers of ϵ and using the symmetry of the phase space. Considering the spectrum of the gluon 1, we find

$$\begin{aligned}
 C_g^{(R)}[\mathcal{Q}] &= \frac{\Phi_{(2)}}{2M} \frac{N}{K} \frac{1}{\mathcal{S}_1} \left[2 \left(\frac{1}{1-x} \right)_+ f_R[\mathcal{Q}](x,0) \right. \\
 &\times \left(-\frac{1}{\epsilon_{\text{coll}}} + 2 \log x \right) + 2x \left(\frac{\log(1-x)}{1-x} \right)_+ f_R[\mathcal{Q}](x,0) \\
 &- \frac{1}{\epsilon} \delta(1-x) \int_0^1 dy [y(1-y)]^{-1-\epsilon} f_R[\mathcal{Q}](x,y) \\
 &\left. + 2 \left(\frac{1}{1-x} \right)_+ \int_0^1 dy \left(\frac{1}{y} \right)_+ f_R[\mathcal{Q}](x,y) \right]. \quad (18)
 \end{aligned}$$

The soft divergences $\sim \delta(1-x)$ cancel by adding the virtual contribution in the same area of the phase space. The last piece of Eq. (18) is a state-dependent finite contribution. The limit $y \rightarrow 0$ corresponds to gluon 1 and gluon 2 becoming collinear 1||2 and the factor 2 in front accounts for the case 1||3. Integration over the phase space gives rise to a pole labelled by ϵ_{coll} and a universal finite part. This divergence is not cancelled by adding the virtual term and reveals that nonperturbative effects are leading in this case. In fact the residual sensitivity can be consistently factorized into the fragmentation function of the gluon into the photon. Such singular residual collinear part corresponds to the first term in Eq. (18) plus the collinear piece of the virtual contribution [$\sim \delta(1-x)$] that comes from the gluon, ghost self-energy loops of the gluon we are selecting, so that it reads

$$\begin{aligned}
 C_g^{(\text{coll})}[\mathcal{Q}] &= -\frac{1}{\epsilon_{\text{coll}}} \left(\frac{4\pi\mu^2}{M^2} \right)^\epsilon \Gamma(1+\epsilon) \frac{\alpha_s}{\pi} \\
 &\times \left\{ 2C_A \left[\frac{x}{(1-x)_+} + \frac{1-x}{x} + x(1-x) \right] \right. \\
 &\left. + \frac{11}{6} C_A \delta(1-x) \right\} \Gamma_{\text{Born}}[\mathcal{Q}]. \quad (19)
 \end{aligned}$$

If we now switch on the light flavors including $q\bar{q}g$ and gluon vacuum polarization diagrams, then we obtain the conventional counterterm $\sim \mathcal{P}_{gg}$, which has to be subtracted at the factorization scale μ_F .

This procedure can be extended to all short-distance terms and may be useful to express the factorization in a more general way. At NLO the individual terms in Eq. (1) may be divergent and will be denoted by tilded quantities. As we have already mentioned, such divergences correspond only to two final partons becoming collinear, and their form is dictated by the factorization theorem. According to this we can reorganize them as follows:

$$\begin{aligned}
 \tilde{C}_\gamma &= C_\gamma + \sum_q C_q \otimes \mathcal{G}_{q \rightarrow \gamma} + C_g \otimes \mathcal{G}_{g \rightarrow \gamma}, \\
 \tilde{C}_q &= \sum_{q'} C_{q'} \otimes \mathcal{G}_{q' \rightarrow q} + C_g \otimes \mathcal{G}_{g \rightarrow q}, \\
 \tilde{C}_g &= \sum_q C_q \otimes \mathcal{G}_{q \rightarrow g} + C_g \otimes \mathcal{G}_{g \rightarrow g}, \quad (20)
 \end{aligned}$$

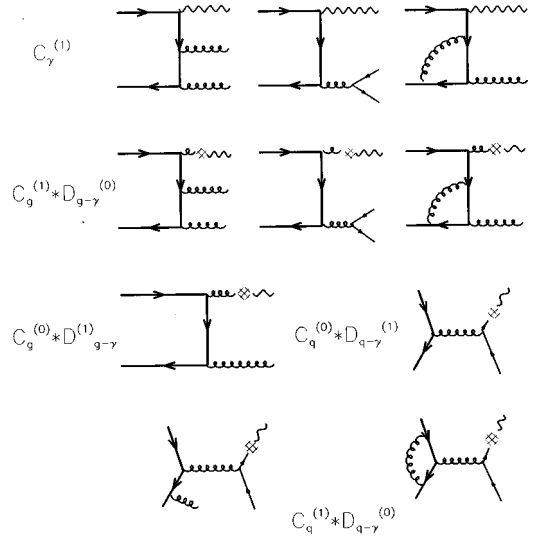


FIG. 3. Sample of NLO Feynman diagrams: direct and fragmentation.

where all of the divergences are now concentrated in the factorization-scale-dependent transition functions $\mathcal{G}_{i \rightarrow j}$:

$$\begin{aligned}
 \mathcal{G}_{a \rightarrow b} &= \delta_{ab} \delta(1-x) + \frac{\alpha_s}{2\pi} \frac{1}{\Gamma(1-\epsilon)} \left(\frac{4\pi\mu^2}{\mu_F^2} \right) \left[-\frac{1}{\epsilon} \mathcal{P}_{ba}(x) \right] \\
 &+ K_{ab}(x), \quad (21)
 \end{aligned}$$

$$\mathcal{G}_{g \rightarrow \gamma} = K_{g\gamma}(x), \quad (22)$$

$$\mathcal{G}_{q \rightarrow \gamma} = \left(\frac{\alpha_{\text{em}} e_q^2}{2\pi} \right) \frac{1}{\Gamma(1-\epsilon)} \left(\frac{4\pi\mu^2}{\mu_F^2} \right)^\epsilon \left[-\frac{1}{\epsilon} \mathcal{P}_{\gamma q} \right] + K_{q\gamma}(x), \quad (23)$$

where $a = g, q, \bar{q}$ and all the coefficients C_i are now finite for $\epsilon \rightarrow 0$. The functions $\mathcal{P}_{ba}(x)$ are the $D=4$ Altarelli-Parisi splitting kernels, collected in Appendix A, and the factors K_{ij} are arbitrary functions, defining the factorization scheme. In this paper we adopt the $\overline{\text{MS}}$ factorization, in which $K_{ij}(x) = 0$ for all i, j . The collinear factors $\mathcal{G}_{i \rightarrow j}$ are usually absorbed into the bare fragmentation functions by defining

$$\begin{aligned}
 D_{q \rightarrow \gamma} &= \mathcal{G}_{q \rightarrow \gamma} + \sum_{q'} \mathcal{G}_{q \rightarrow q'} \otimes D_{q' \rightarrow \gamma}^B + \mathcal{G}_{q \rightarrow g} \otimes D_{g \rightarrow \gamma}^B, \\
 D_{g \rightarrow \gamma} &= \mathcal{G}_{g \rightarrow \gamma} + \sum_q \mathcal{G}_{g \rightarrow q} \otimes D_{q \rightarrow \gamma}^B + \mathcal{G}_{g \rightarrow g} \otimes D_{g \rightarrow \gamma}^B, \quad (24)
 \end{aligned}$$

so that we can write the physical decay rate in terms of finite quantities

$$\frac{d\Gamma}{dz}(\gamma+X) = C_\gamma + \sum_q C_q \otimes D_{q \rightarrow \gamma} + C_g \otimes D_{g \rightarrow \gamma}. \quad (25)$$

As illustrated in Fig. 3, we write the general structure of the NLO processes as

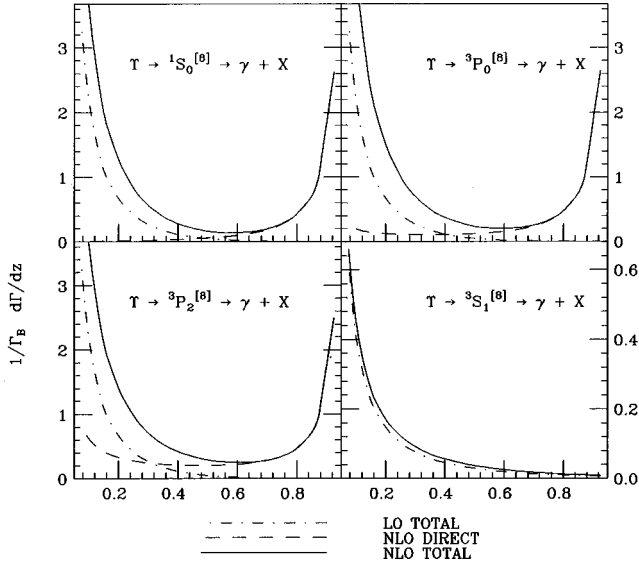


FIG. 4. Different color-octet contributions to the photon spectrum in the Y decay up to $O(v^4)$. The differential decay widths $d\Gamma/dz$ are reported as a function of $z = E_\gamma/m$. All the distributions displayed are normalized to the respective Born (that is $Q \rightarrow g\gamma\gamma$ for C -even and ${}^3S_1^{[8]} \rightarrow q\bar{q}$ for the only C -odd contribution).

$$\frac{d\Gamma^{(1)}}{dz} = \sum_Q [C_\gamma^{(1)}[Q] + C_g^{(1)}[Q] \otimes D_{g \rightarrow \gamma}^{(0)} + C_g^{(0)}[Q] \otimes D_{g \rightarrow \gamma}^{(1)} + 2C_q^{(1)}[Q] \otimes D_{q \rightarrow \gamma}^{(0)} + 2C_q^{(0)}[Q] \otimes D_{q \rightarrow \gamma}^{(1)}]. \quad (26)$$

Different color-octet contributions to the photon spectrum are shown in Fig. 4.

IV. RESULTS

In the previous section we have shown how the short-distance coefficients have been calculated and all the final-state collinear divergences have been consistently absorbed into fragmentation functions. Now, in order to investigate the phenomenological applications of color-octet states, an estimate of the NRQCD matrix elements (ME) must be given. The long-distance MEs can be calculated on the lattice, extracted from experiments when enough data are available, or roughly determined by using scaling rules of NRQCD or by renormalization group (RG) arguments. At the present time none of the aforementioned techniques is able to give a set of precise values for MEs and, as we will see below, estimates are affected by large uncertainties.

Let us start our analysis by studying if the experimental data on total and leptonic decay rates of the bottomonium can provide useful bounds on the matrix elements which appear in the radiative decays. To NLO accuracy in v , we can write

$$\Gamma(Y \rightarrow l^+l^-) = c_{ll}({}^3S_1^{[1]}) \langle Y | \mathcal{O}_1({}^3S_1) | Y \rangle + d_{ll}({}^3S_1^{[1]}) \langle Y | \mathcal{P}_1({}^3S_1) | Y \rangle \quad (27)$$

and

$$\begin{aligned} \Gamma(Y \rightarrow LH) = & c_1({}^3S_1^{[1]}) \langle Y | \mathcal{O}_1({}^3S_1) | Y \rangle \\ & + d_1({}^3S_1^{[1]}) \langle Y | \mathcal{P}_1({}^3S_1) | Y \rangle \\ & + c_8({}^3S_1^{[8]}) \langle Y | \mathcal{O}_8({}^3S_1) | Y \rangle \\ & + c_8({}^1S_0^{[8]}) \langle Y | \mathcal{O}_8({}^1S_0) | Y \rangle \\ & + \sum_J c_8({}^3P_J^{[8]}) \langle Y | \mathcal{O}_8({}^3P_J) | Y \rangle. \quad (28) \end{aligned}$$

The short distance coefficients c_{ll}, c_1, c_8 are known to NLO accuracy in α_s [16,17,11] while d_{ll}, d_1 have been calculated numerically and analytically in Refs. [18,15]. Using heavy-quark spin symmetry [4] which is valid up to corrections of order v^2 , and the equations of motion of NRQCD [15], one can reduce the number of independent MEs to 4: $\langle Y | \mathcal{O}_1({}^3S_1) | Y \rangle$, $\langle Y | \mathcal{O}_8({}^1S_0) | Y \rangle$, $\langle Y | \mathcal{O}_8({}^3S_1) | Y \rangle$, $\langle Y | \mathcal{O}_8({}^3P_0) | Y \rangle$.

Even if there is no possibility to obtain values for each ME separately, one can still hope that the same linear combination of color-octet MEs appears in the radiative decays. Indeed this is the case only for the following combination:

$$\mathcal{M}_7 \equiv \langle Y | \mathcal{O}_8({}^1S_0) | Y \rangle + 7 \frac{\langle Y | \mathcal{O}_8({}^3P_0) | Y \rangle}{m^2}, \quad (29)$$

which contributes at LO in both the decays and it is still maintained with a good approximation at NLO (see Ref. [11] and Fig. 4). This reduces the free parameters to three and allows to constraint at most a linear combination of \mathcal{M}_7 and $\langle Y | \mathcal{O}_8({}^3S_1) | Y \rangle$. We have to conclude that the information we can extract from the total decay rates is not sufficient on its own to allow a prediction for the radiative decays. Nevertheless we will use this information to check if estimates of the MEs obtained with other methods are compatible with the experimental data.

A further possibility is given by the power counting techniques of NRQCD. The velocity-scaling of the MEs is basically determined by the number of derivatives in the respective operators and by the number of electric or magnetic dipole transitions between the $Q\bar{Q}$ pair annihilated at short distance and the $Q\bar{Q}$ pair in the asymptotic physical state. This can nicely be described by a multipole expansion of the nonperturbative transition $Y \rightarrow Q$: ${}^1S_0^{[8]}$ can be reached by a chromomagnetic dipole transition, ${}^3S_1^{[8]}$ by a double chromoelectric emission, and ${}^3P_J^{[8]}$ by a simple chromoelectric transition. The first two are of order v^4 while the last only of order v^2 . Finally, since the hard-production vertex for a P wave is already suppressed by v^2 relative to the production of an S state, one realizes that the color-octet C -even states and ${}^1S_0^{[8]}$ all contribute at the same order in v . Following this approach, we can write

$$\begin{aligned} \langle Y | \mathcal{O}_8({}^3S_1) | Y \rangle & \approx v^4 \langle Y | \mathcal{O}_1({}^3S_1) | Y \rangle, \\ \langle Y | \mathcal{O}_8({}^3P_J) | Y \rangle & \approx m^2 v^4 \langle Y | \mathcal{O}_1({}^3S_1) | Y \rangle, \quad (30) \end{aligned}$$

where for bottomonium one usually takes $v^2 \simeq 0.1$ and $m \simeq 4.8$ GeV.

An alternative approach has been considered by Gremm and Kapustin in Ref. [15]. They obtain estimates for the color-octet operators by solving the RG equations [4]. To order v^4 and leading order in α_s , they read

$$\Lambda \frac{d}{d\Lambda} \langle Y | \mathcal{O}_8(^1S_0) | Y \rangle = O(\alpha_s v^6), \quad (31)$$

$$\Lambda \frac{d}{d\Lambda} \langle Y | \mathcal{O}_8(^3S_1) | Y \rangle = \frac{24B_F\alpha_s}{\pi m^2} \langle Y | \mathcal{O}_8(^3P_0) | Y \rangle, \quad (32)$$

$$\Lambda \frac{d}{d\Lambda} \langle Y | \mathcal{O}_8(^3P_0) | Y \rangle = \frac{8C_F\alpha_s}{81\pi} (M_Y - 2m)^2 \times \langle Y | \mathcal{O}_1(^3S_1) | Y \rangle, \quad (33)$$

where we used the heavy quark spin symmetry to reexpress the expectation values of $\mathcal{O}_8(^3P_{1,2})$ in terms of $\mathcal{O}_8(^3P_0)$. We note here that our normalization for the color-singlet NRQCD operators differs from the original one introduced by BBL, i.e., $\mathcal{O}_1 = (1/2N_c)\mathcal{O}_1^{\text{BBL}}$. Equation (32) differs from the respective equations that appear in Ref. [15] because we included the contribution of $^3P_1^{[8]}$ to the evolution of $\mathcal{O}_8(^3S_1)$, which was left out in the previous treatment.² Assuming that logarithmic terms of the evolution are dominant [4,15] over the MEs evaluated at a starting scale $\Lambda \sim \Lambda_{\text{QCD}}$, we obtain

$$\begin{aligned} \langle Y | \mathcal{O}_8(^3S_1) | Y \rangle_{\text{RG}} &\approx \frac{32B_FC_F}{27} \left(\frac{M_Y - 2m}{m} \right)^2 \\ &\times \left[\frac{1}{b_0} \log \left(\frac{1}{\alpha_s(m)} \right) \right]^2 \langle Y | \mathcal{O}_1(^3S_1) | Y \rangle, \end{aligned} \quad (34)$$

$$\begin{aligned} \langle Y | \mathcal{O}_8(^3P_0) | Y \rangle_{\text{RG}} &\approx \frac{8C_F}{81} (M_Y - 2m)^2 \frac{1}{b_0} \\ &\times \log \left(\frac{1}{\alpha_s(m)} \right) \langle Y | \mathcal{O}_1(^3S_1) | Y \rangle, \end{aligned} \quad (35)$$

$$\langle Y | \mathcal{O}_8(^1S_0) | Y \rangle_{\text{RG}} \approx 0. \quad (36)$$

Once numbers are plugged into the previous expression, one realizes that MEs in Eqs. (30) result larger by more than one order of magnitude with respect to the RG estimates shown in Eqs. (34)–(36). This suggests that the very first assumption, i.e., that the nonperturbative matrix elements should be dominated by QCD evolution, is doubtful and can-

²The authors of Ref. [15] agree that it is correct to include the $^3P_1^{[8]}$ contribution in the right-hand side of Eq. (32) (private communication).

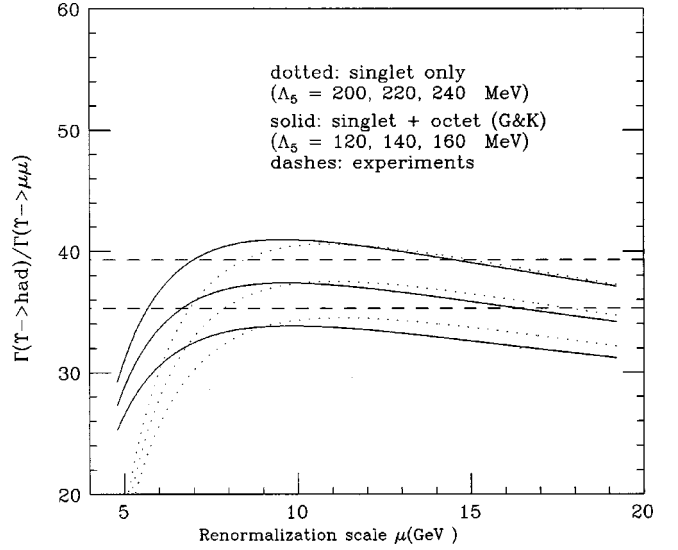


FIG. 5. Ratio $\Gamma(Y \rightarrow \text{had})/\Gamma(Y \rightarrow \mu^+ \mu^-)$ versus renormalization scale μ for different values of Λ_5 . The solid lines include NLO color-octet contributions with the RG estimates of the matrix elements. The dotted lines include color-singlet only.

not be justified unless their input values were accidentally much smaller than the “natural” values given in Eqs. (30). At this level the above assumption has to be considered as a definition of a model. In order to obtain an independent test on the above MEs, it is useful to verify that the RG estimates are compatible with the bounds from total and leptonic decay rates discussed previously. To this aim we have analyzed their impact on the observable $R_\mu(Y) = \Gamma(Y \rightarrow \text{had})/\Gamma(Y \rightarrow \mu^+ \mu^-)$. The use of this quantity is particularly advantageous because of the cancellation of several sources of uncertainties: both the color-singlet NRQCD matrix element and the overall dependence on the bottom mass cancel in the ratio. As a result the mass enters only in the logarithm of the renormalization scale and its uncertainties can be naturally associated to the choice of the scale itself.

In Fig. 5, the ratio R_μ is plotted versus the renormalization scale μ (i.e., the NRQCD factorization scale is kept equal to the renormalization one); $\Gamma_{\mu\mu}$ and Γ_{had} are given in Eqs. (27) and (28). The dashed lines limit the 2σ band of the experimental value of $R_\mu = 37.3 \pm 1.0$ [19]. The theoretical curves are drawn according to the following choice of parameters: $v^2 = 0.1$ and $\alpha_{\text{em}}(m_b) = 1/132$. Hence Fig. 5 shows that, once the colour-octet RG MEs estimation is plugged in, the ratio R_μ is consistent with the experiments only for $\Lambda_5 \simeq 140$ MeV [$\alpha_s(M_Z) \simeq 0.110$]. On the other hand if we drop the color-octet term, just the NLO color-singlet contribution can still reproduce the experimental measure of R_μ by choosing a much higher value of Λ_5 , namely, $\Lambda_5 \simeq 220$ MeV [$\alpha_s(M_Z) \simeq 0.118$].

Now we fix the renormalization scale $\mu_R = 10$ GeV. We note that, more than corresponding to the “natural” choice $\mu_R \simeq M_Y$, this value also satisfies the so-called “minimal sensitivity principle” [20], i.e., it is the value at which $\mu_R(d/d\mu_R)R_\mu(\mu_R)$ vanishes. Within this choice, we plot the ratio R_μ versus the variable

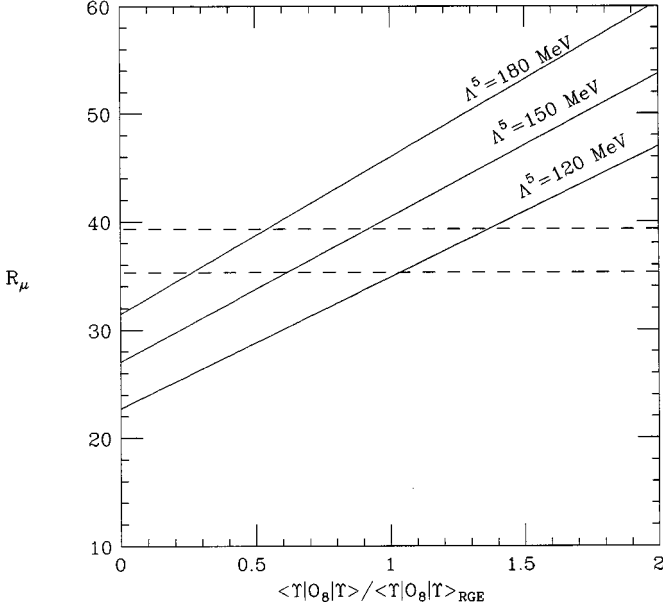


FIG. 6. Ratio $\Gamma(Y \rightarrow \text{had})/\Gamma(Y \rightarrow \mu^+ \mu^-)$ versus color-octet matrix elements for different values of Λ_5 . The dashed lines indicate the 2σ interval of the experimental value for R_μ .

$$x = \frac{\langle Y | \mathcal{O}_8(^3P_0) | Y \rangle}{\langle Y | \mathcal{O}_8(^3P_0) | Y \rangle_{\text{RG}}} = \frac{\langle Y | \mathcal{O}_8(^3S_1) | Y \rangle}{\langle Y | \mathcal{O}_8(^3S_1) | Y \rangle_{\text{RG}}}. \quad (37)$$

The result is shown in Fig. 6. The solid lines represent the theoretical calculation of R_μ and the dashed lines are the 2σ experimental range, as in Fig. 5. The larger the color-octet MEs are, the smaller Λ_5 has to be taken. In particular, already for values of the MEs of the order of twice the RG estimates, we would find a value of $\Lambda_5 \approx 80 \text{ MeV}$ [$\alpha_s(M_Z) \approx 0.102$], well outside the present world average range.

Following this line one finds that the MEs provided by the velocity scaling rules are strictly excluded. In an ideal global fit perspective both the value of Λ_5 and the color-octet MEs should be extracted from the data. Unfortunately, as we have explicitly shown previously, the experimental inputs in the Y decay sector are not sufficient to perform a fit of such a large number of unknown parameters.

As a confirmation of what we found in Figs. 5 and 6 shows that the RG estimate reproduces the experimental value of R_μ for $\Lambda_5 \approx 140 \text{ MeV}$. Such a value of Λ_5 corresponds to $\alpha_s(m_b) \approx 0.190$ and $\alpha_s(M_Z) \approx 0.110$. The world average of α_s [$\alpha_s(M_Z) = 0.119 \pm 0.004$] (or equivalently $\Lambda_5 \approx 237 \text{ MeV}$) is actually consistent with a vanishing (or even negative) octet contribution to the Y decay into hadrons. Nevertheless the uncertainties involved are still large: NNLO QCD corrections (reflected in the μ dependence of the NLO correction) might be important as well as higher twist effects. A clear indication that higher order effects are not negligible, comes from the two-loop calculation of the leptonic width recently performed by Beneke *et al.* [21]: in this case, it is found that the $\mathcal{O}(\alpha_s^2)$ corrections (NNLO) are of the same size (or even larger) of the NLO ones.

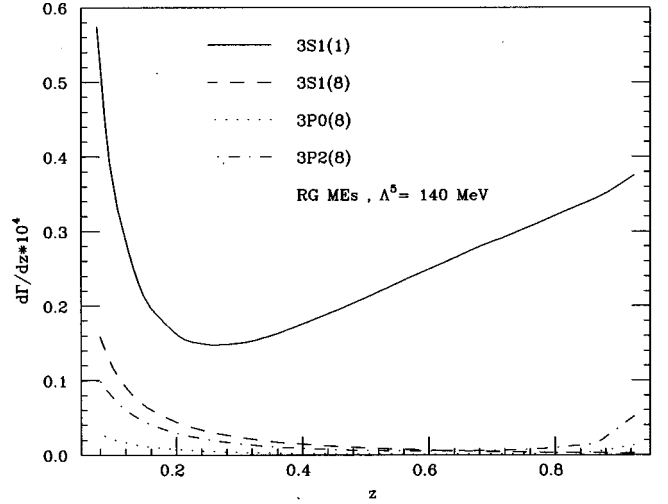


FIG. 7. Various Fock contributions to the photon spectrum as a function of $z = E_\gamma/m$. The solid line gives the LO singlet contribution. Fragmentation and NLO direct are summed up for each color-octet state. The NRQCD MEs are related to the color-singlet one through the RG estimate. The color-singlet matrix element is arbitrarily chosen to be $\langle Y | \mathcal{O}_1(^3S_1) | Y \rangle = M^2/4\pi$, so that comparison with Ref. [5] is straightforward.

Summing up, we can say that even if comparison with scaling rules of NRQCD shows that RG estimates are sizeably smaller than expected, consistency between theory and experiment in total decay rates strongly disfavor much larger color-octet MEs. We then conclude that the RG estimates of the color-octet MEs, are the most reasonable at the present stage of our knowledge.

In Fig. 4 we show in detail the contribution of the single color-octet components. The figure reports LO, direct, and full NLO contributions for states normalized to their respective Born decay widths at $\mathcal{O}(\alpha_s \alpha_{\text{em}})$. Let us consider the C -even states first ($^1S_0^{[8]}$, $^3P_0^{[8]}$, $^3P_2^{[8]}$). It is evident that they contribute to the spectrum with a very similar shape: there is a strong enhancement at low values of z due to the fragmentation contribution that is present both at LO and NLO. Then it is clearly seen that direct photons mainly contribute near the end-point, a zone of the spectrum where the fixed-order calculation is not reliable: in fact there are clear indications of a need of resummation both in the short-distance perturbative expansion in α_s and in the long-distance v series. In Ref. [7] Rothstein and Wise identified an infinite class of NRQCD operators, which determine the shape of photonic end-point functions, and introduced the so-called ‘‘shape function,’’ to be extracted from data. The overall effect of color-octet states would be a smearing of the energy distribution near the end point on the interval $v^2 \approx 0.1$. In the case of the $^3S_1^{[8]}$ component, the direct amplitude is not divergent in $z=1$ and the NLO correction to the LO fragmentation picture is very small. Indeed the NLO contribution from direct photons is negative in the $\overline{\text{MS}}$ -renormalization scheme and is almost balanced by the other NLO fragmentation terms.

Finally Figs. 7 and 8 show the total contribution to the spectrum, using the RG estimate for the nonrelativistic ma-

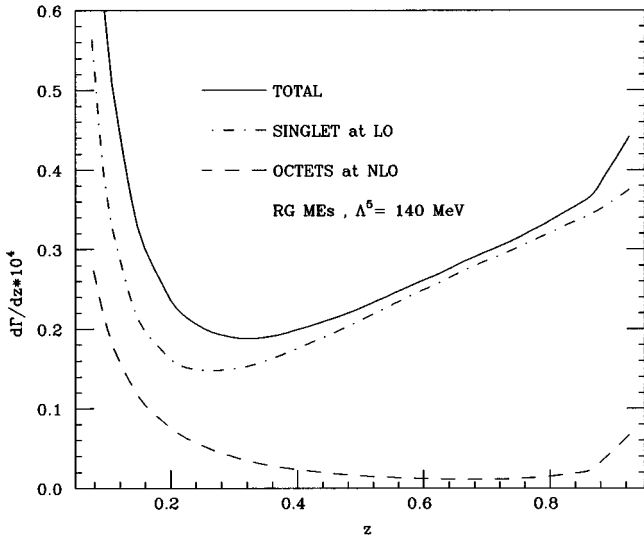


FIG. 8. Total color-octet contribution on the LO, color-singlet photon spectrum. Notice that neither NLO QCD nor relativistic effects are included in the singlet contribution. Normalization and MEs as in Fig. 7.

trix elements. We notice that the overall effect of octet states is at its minimum in the central region of the spectrum, exactly where the singlet LO direct contribution dominates. This indicates that this region of the spectrum is “safe” from color-octet effects, and therefore we think that it should be used to make a comparison with experimental data. Moreover this indicates that relativistic corrections to the singlet (which are indeed important) and higher-order strong ones should be included to have a consistent theoretical picture at NLO. On the other side, for small values of z , color-octet components are not negligible. In this area of the phase space, the fragmentation components from gluons contribute at the same order in α_s as the ones from quarks, and there is no signature to distinguish between the two. Contrary to LO expectations in the framework of CSM [5], we conclude that the decay of Υ into a photon would not be useful for an estimate of the photon fragmentation functions.

As a final remark, we notice that, not surprisingly, many of the aspects of the photon spectrum in quarkonium decay, resemble those in photoproduction [22,23]. Cross sections plotted versus the inelasticity z of the quarkonium state show a very similar pattern: for $z \approx 1$, a divergence, which is not supported by the available experimental data, reveals the breaking of the NRQCD expansion in powers of α_s and v . On the other side, for low values of z , the resolved contributions, which corresponds to fragmentation in the decays, are indeed dominated by color-octet states.

V. CONCLUSIONS

We presented the calculation of $\mathcal{O}(\alpha_s^2 \alpha_{\text{em}})$ color-octet corrections to the decay of Υ into one photon plus light hadrons. Both direct and fragmentation contributions have been included at NLO. In order to study the impact of these contributions on the photon spectrum, an estimate of the

nonperturbative MEs was also given. By comparing the available experimental data on fully inclusive and leptonic decay rates with the NLO theoretical predictions of NRQCD, we found an unexpected result: estimates based on naive scaling rules result in large color-octet contributions to the total rates which are not consistent with the data. In particular, it turns out that nonperturbative MEs should be much smaller than expected from NRQCD scaling rules. Nevertheless, using the above mentioned estimates for the nonperturbative MEs, we showed that there are sizeable effects at the end points of the spectrum of the photon. In the case of low values of z , the possibility of measuring the fragmentation function of a gluon into a photon, which was suggested by the LO result in the CSM [5], becomes unfeasible: for the color-octet states both quark and gluon fragmentation processes are of the same order in $\alpha_s \alpha_{\text{em}}$ and there is no signature to distinguish between the two. Moreover, for values of z near the end point, breaking of the fixed-order calculation is manifest, and the resummations of both short-distance coefficient in α_s and nonperturbative MEs in v , are called for. Nevertheless a “safe” region, for $0.3 < z < 0.9$, has been found where octet effects are at their minimum and the perturbative expansion in powers of α_s and v under proper control. Following this point of view, we consider the NLO QCD correction the color-singlet differential decay $d\Gamma/dE_\gamma(\Upsilon \rightarrow {}^3S_1^{[1]} \rightarrow \gamma gg)$ worth while to be undertaken.

ACKNOWLEDGMENTS

It is a pleasure to thank M. L. Mangano for valuable advice, discussions, and suggestions during all the stages of this work. We thank L. Bourhis for providing us with a ready-to-use set of photon fragmentation functions. Moreover, we are grateful to M. Beneke and G. T. Bodwin for reading the manuscript and for their useful suggestions. This work was supported in part by the EU Fourth Framework Programme “Training and Mobility of Researchers,” network “Quantum Chromodynamics and the Deep Structure of Elementary Particles,” Contract No. FMRX-CT98-0194 (DG 12-MIHT), and partially by the U.S. Department of Energy, under Contract No. W-31-109-ENG-38.

APPENDIX A: SYMBOLS AND NOTATION

This appendix collects the meaning of various symbols, which are used throughout the paper.

Kinematical factors:

$$M = 2m, \quad v = \sqrt{1 - \frac{M^2}{s}}, \quad (\text{A1})$$

where s is the partonic center-of-mass energy squared and S_{had} is the hadronic one; v is the velocity of the bound (anti)quark in the quarkonium rest frame, $2v$ then being the relative velocity of the quark and the antiquark. The following expression is used:

$$f_\epsilon(Q^2) = \left(\frac{4\pi\mu^2}{Q^2} \right)^\epsilon \Gamma(1+\epsilon) \quad [T(x)]_+ = [T(x)]_a - \delta(1-x) \int_0^a T(x) dx. \quad (\text{A15})$$

$$= 1 + \epsilon \left(-\gamma_E + \log(4\pi) + \log \frac{\mu^2}{Q^2} \right) + \mathcal{O}(\epsilon^2). \quad (\text{A2})$$

Altarelli-Parisi splitting functions. Several functions related to the AP splitting kernels enter in our calculations. We collect here our definitions:

$$P_{qq}(x) = C_F \left[\frac{1+x^2}{1-x} - \epsilon(1-x) \right], \quad (\text{A3})$$

$$\mathcal{P}_{qq}(x) = C_F \left[\frac{1+x^2}{(1-x)_+} + \frac{3}{2} \delta(1-x) \right], \quad (\text{A4})$$

$$P_{qg}(x) = T_F [x^2 + (1-x)^2 - 2\epsilon x(1-x)], \quad (\text{A5})$$

$$\mathcal{P}_{qg}(x) = T_F [x^2 + (1-x)^2], \quad (\text{A6})$$

$$P_{\gamma q}(x) = \frac{1+(1-x)^2}{x} - \epsilon x, \quad (\text{A7})$$

$$\mathcal{P}_{\gamma q}(x) = \frac{1+(1-x)^2}{x}, \quad (\text{A8})$$

$$P_{gq}(x) = C_F \left[\frac{1+(1-x)^2}{x} - \epsilon x \right], \quad (\text{A9})$$

$$\mathcal{P}_{gq}(x) = C_F \left[\frac{1+(1-x)^2}{x} \right], \quad (\text{A10})$$

$$P_{gg}(x) = 2C_A \left[\frac{x}{1-x} + \frac{1-x}{x} + x(1-x) \right], \quad (\text{A11})$$

$$\mathcal{P}_{gg}(x) = 2C_A \left[\frac{x}{(1-x)_+} + \frac{1-x}{x} x + x(1-x) \right] + b_0 \delta(1-x). \quad (\text{A12})$$

The P_{ij} are the D -dimensional splitting functions that appear in the factorization of collinear singularities from real emission, while the functions \mathcal{P}_{ij} are the four-dimensional AP kernels, which enter in the $\overline{\text{MS}}$ collinear counter-terms. The $+$ and a distributions are defined by

$$\int_0^1 dx [T(x)]_+ \phi(x) = \int_0^1 dx T(x) [\phi(x) - \phi(1)], \quad (\text{A13})$$

$$\int_a^1 dx [T(x)]_a \phi(x) = \int_a^1 dx T(x) [\phi(x) - \phi(1)], \quad (\text{A14})$$

where $T(x)$ is the function associated to the distributions $[T(x)]_{+,a}$. We recall a useful weak distributional identity,

In particular it is straightforward to get

$$\left(\frac{1}{1-x} \right)_+ = \left(\frac{1}{1-x} \right)_a + \delta(1-x) \log(1-a), \quad (\text{A16})$$

$$\left(\frac{\log(1-x)}{1-x} \right)_+ = \left(\frac{\log(1-x)}{1-x} \right)_a + \delta(1-x) \frac{1}{2} \log^2(1-a). \quad (\text{A17})$$

Color coefficients:

$$C_F = \frac{N_c^2 - 1}{2N_c}, \quad C_A = N_c, \quad B_F = \frac{N_c^2 - 4}{4N_c}, \quad T_F = \frac{1}{2}. \quad (\text{A18})$$

The following standard symbol is used:

$$b_0 = \frac{11}{6} C_A - \frac{2}{3} T_F n_f, \quad (\text{A19})$$

with n_f the number of flavors lighter than the bound one.

NRQCD operators. To denote a perturbative $Q\bar{Q}$ state with generic spin and angular momentum quantum numbers, and in a color-singlet or color-octet state, we use the symbol

$$Q^{[1,8]} \equiv Q\bar{Q} [^{2S+1}L_J^{[1,8]}]. \quad (\text{A20})$$

Notice that, according to the discussion in Ref. [11], our conventions differ from the Bodwin, Braaten, and Lepage ones [4] (labeled here as BBL) in the case of a color-singlet:

$$\mathcal{O}_1 = \frac{1}{2N_c} \mathcal{O}_1^{\text{BBL}}, \quad (\text{A21})$$

$$\mathcal{O}_8 = \mathcal{O}_8^{\text{BBL}}. \quad (\text{A22})$$

APPENDIX B: SUMMARY OF LOWEST ORDER RESULTS

1. Born widths

The decay rates read

$$\Gamma(Y \rightarrow Q^{[1,8]} \rightarrow ab) = \hat{\Gamma}(Q^{[1,8]} \rightarrow ab) \langle Y | \mathcal{O}_{[1,8]}(^{2S+1}L_J) | Y \rangle, \quad (\text{B1})$$

the short-distance coefficients $\hat{\Gamma}$ having been calculated according to the rules of Ref. [11]. We shall use the short-hand notation

$$\Gamma(Q^{[1,8]} \rightarrow ab) \equiv \Gamma(Y \rightarrow Q^{[1,8]} \rightarrow ab) \quad (\text{B2})$$

to indicate the decay of the physical quarkonium state H through the intermediate $Q\bar{Q}$ state $Q^{[1,8]} = Q\bar{Q} [^{2S+1}L_J^{[1,8]}]$. The D -dimensional ($D = 4 - 2\epsilon$) $O(\alpha_s, \alpha_{\text{em}})$ level decay rates read

$$\Gamma_{\text{Born}}(^1S_0^{[8]} \rightarrow g\gamma) = \frac{32\alpha_s\alpha_{\text{em}}e_Q^2\mu^4\pi^2}{m^2}\Phi_{(2)}(1-\epsilon)(1-2\epsilon) \times \langle Y | \mathcal{O}_8(^1S_0) | Y \rangle, \quad (\text{B3})$$

$$\Gamma_{\text{Born}}(^3S_1^{[8]} \rightarrow g\gamma) = 0, \quad (\text{B4})$$

$$\Gamma_{\text{Born}}(^3P_0^{[8]} \rightarrow g\gamma) = \frac{288\alpha_s\alpha_{\text{em}}e_Q^2\mu^4\pi^2}{m^4} \times \Phi_{(2)}\frac{1-\epsilon}{3-2\epsilon} \langle Y | \mathcal{O}_8(^3P_0) | Y \rangle, \quad (\text{B5})$$

$$\Gamma_{\text{Born}}(^3P_1^{[8]} \rightarrow g\gamma) = 0, \quad (\text{B6})$$

$$\Gamma_{\text{Born}}(^3P_2^{[8]} \rightarrow g\gamma) = \frac{64\alpha_s\alpha_{\text{em}}e_Q^2\mu^4\pi^2}{m^4} \times \Phi_{(2)}\frac{(6-13\epsilon+4\epsilon^2)}{(3-2\epsilon)(5-2\epsilon)} \times \langle Y | \mathcal{O}_8(^3P_2) | Y \rangle. \quad (\text{B7})$$

Lowest $\mathcal{O}(\alpha_s^2)$ contributions:

$$\Gamma_{\text{Born}}(^1S_0^{[8]} \rightarrow gg) = B_F \frac{16\alpha_s^2\mu^4\pi^2}{m^2} \Phi_{(2)}(1-\epsilon)(1-2\epsilon) \langle Y | \mathcal{O}_8(^1S_0) | Y \rangle, \quad (\text{B8})$$

$$\Gamma_{\text{Born}}(^3S_1^{[8]} \rightarrow q\bar{q}) = 8 \frac{\alpha_s^2\mu^4\pi^2}{m^2} \Phi_{(2)}\frac{1-\epsilon}{3-2\epsilon} \langle Y | \mathcal{O}_8(^3S_1) | Y \rangle, \quad (\text{B9})$$

$$\Gamma_{\text{Born}}(^3P_0^{[8]} \rightarrow gg) = B_F \frac{144\alpha_s^2\mu^4\pi^2}{m^4} \Phi_{(2)}\frac{(1-\epsilon)}{(3-2\epsilon)} \langle Y | \mathcal{O}_8(^3P_0) | Y \rangle, \quad (\text{B10})$$

$$\Gamma_{\text{Born}}(^3P_1^{[8]} \rightarrow gg) = 0, \quad (\text{B11})$$

$$\Gamma_{\text{Born}}(^3P_2^{[8]} \rightarrow gg) = B_F \frac{32\alpha_s^2\mu^4\pi^2}{m^4} \Phi_{(2)}\frac{(6-13\epsilon+4\epsilon^2)}{(3-2\epsilon)(5-2\epsilon)} \langle Y | \mathcal{O}_8(^3P_2) | Y \rangle, \quad (\text{B12})$$

where $\Phi_{(2)}$ is defined according to Eq. (14).

2. The LO spectrum coefficients $C^{(0)}[\mathcal{Q}]$

We can now read out the lowest-order coefficients according to Eqs. (5)–(11). For $\mathcal{Q} = ^3P_j^{[8]}$, $^1S_0^{[8]}$ we have

$$C_\gamma^{(0)}[\mathcal{Q}](z) = \Gamma_{\text{Born}}[\mathcal{Q} \rightarrow g\gamma] \delta(1-z), \quad (\text{B13})$$

$$C_g^{(0)}[\mathcal{Q}](x) = 2\Gamma_{\text{Born}}[\mathcal{Q} \rightarrow gg] \delta(1-x), \quad (\text{B14})$$

$$C_q^{(0)}[\mathcal{Q}](x) = 0, \quad (\text{B15})$$

and, for $^3S_1^{[8]}$,

$$C_\gamma^{(0)}[^3S_1^{[8]}](z) = 0, \quad (\text{B16})$$

$$C_g^{(0)}[^3S_1^{[8]}](x) = 0, \quad (\text{B17})$$

$$C_q^{(0)}[^3S_1^{[8]}](x) = \Gamma_{\text{Born}}[\mathcal{Q} \rightarrow q\bar{q}] \delta(1-x). \quad (\text{B18})$$

APPENDIX C: SUMMARY OF $\mathcal{O}(\alpha_s^2\alpha_{\text{em}})$ RESULTS

1. The NLO photonic coefficients $C_\gamma^{(1)}[\mathcal{Q}]$

We summarize the NLO spectrum coefficient following the convention of Eqs. (5)–(26). The photon energy fraction is $z = E_\gamma/m$. Components $\sim \delta(z)$ have been neglected. For $\mathcal{Q} = ^1S_0^{[8]}$, $^3P_0^{[8]}$, $^3P_2^{[8]}$, we have

$$C_\gamma^{(1)}[\mathcal{Q}] = \frac{\alpha_s}{2\pi} \Gamma_{\text{Born}}[\mathcal{Q} \rightarrow g\gamma] \times \left[\left(A[\mathcal{Q}] + 2b_0 \log \frac{\mu_R}{2m} \right) \delta(1-z) + \left(\frac{1}{1-z} \right)_+ f_1^+[\mathcal{Q}](z) + \left(\frac{\log(1-z)}{1-z} \right)_+ f_2^+[\mathcal{Q}](z) \right], \quad (\text{C1})$$

where

$$A[^1S_0^{[8]}] = C_F \left(-10 + \frac{\pi^2}{2} \right) + C_A \left(\frac{121}{18} - \frac{\pi^2}{2} \right) - \frac{10}{9} n_f T_F, \quad (\text{C2})$$

$$A[^3P_0^{[8]}] = C_F \left(-\frac{14}{3} + \frac{\pi^2}{2} \right) + C_A \left(\frac{85}{18} - \frac{\pi^2}{2} \right) - \frac{10}{9} n_f T_F, \quad (\text{C3})$$

$$A[^3P_2^{[8]}] = -8C_F + C_A \left(\frac{47}{9} + \log 2 \right) - \frac{8}{45} n_f T_F, \quad (\text{C4})$$

and

$$f_1^\gamma[{}^1S_0^{[8]}](z) = C_A \frac{(-72 + 144z - 176z^2 + 104z^3 - 23z^4)}{6(-2+z)^2 z} + n_f T_F \frac{2}{3} z, \quad (\text{C5})$$

$$f_1^\gamma[{}^3P_0^{[8]}](z) = C_A \frac{1}{54(-2+z)^4 z^3} (-960 + 3360z - 6224z^2 + 5312z^3 - 1544z^4 - 520z^5 + 496z^6 - 136z^7 + 9z^8) + n_f T_F \frac{2}{27z} (z+2)^2, \quad (\text{C6})$$

$$f_1^\gamma[{}^3P_2^{[8]}](z) = C_A \frac{1}{36(-2+z)^4 z^3} (-240 + 1848z - 7820z^2 + 13976z^3 - 12710z^4 + 6254z^5 - 1628z^6 + 197z^7 - 15z^8) + n_f T_F \frac{1}{9z} (10 - 5z + z^2), \quad (\text{C7})$$

$$f_2^\gamma[{}^1S_0^{[8]}](z) = C_A \frac{2(+12 - 36z + 56z^2 - 52z^3 + 28z^4 - 8z^5 + z^6)}{(-2+z)^3 z^2}, \quad (\text{C8})$$

$$f_2^\gamma[{}^3P_0^{[8]}](z) = C_A \frac{2}{9(-2+z)^5 z^4} (+160 - 720z + 1624z^2 - 2016z^3 + 1360z^4 - 468z^5 + 104z^6 - 66z^7 + 40z^8 - 10z^9 + z^{10}), \quad (\text{C9})$$

$$f_2^\gamma[{}^3P_2^{[8]}](z) = C_A \frac{1}{3(-2+z)^5 z^4} (+40 - 348z + 1618z^2 - 3684z^3 + 4702z^4 - 3669z^5 + 1826z^6 - 582z^7 + 115z^8 - 13z^9 + z^{10}). \quad (\text{C10})$$

For the ${}^3S_1^{[8]}$ component we obtain

$$C_\gamma^{(1)}[{}^3S_1^{[8]}] = \frac{20\alpha_{\text{em}} e_Q^2 \alpha_s^2}{9} \left[\frac{1}{z(-2+z)^2} (8 - 12z + 7z^2 - 2z^3) + \frac{2}{(-2+z)^3 z^2} (-1+z)(8 - 12z + 5z^2) \log(1-z) \right] \frac{\langle Y | \mathcal{O}_8[{}^3S_1] | Y \rangle}{m^2} + \Gamma_{\text{Born}}({}^3S_1^{[8]} \rightarrow q\bar{q}) \frac{\alpha_{\text{em}}}{\pi} P_{\gamma q}(z) \left(\log \frac{4m^2}{\mu_F^2} + \log(1-z) + 2 \log z \right) \sum_q e_q^2, \quad (\text{C11})$$

and finally for ${}^3P_1^{[8]}$,

$$C_\gamma^{(1)}[{}^3P_1^{[8]}] = \frac{2\alpha_{\text{em}} e_Q^2 \alpha_s^2}{3} \left[\frac{1}{(-2+z)^4 z^3} (240 + 312z - 2620z^2 + 4204z^3 - 3150z^4 + 1260z^5 - 276z^6 + 31z^7) + \frac{12}{(-2+z)^5 z^4} (-1+z)(40 + 52z - 430z^2 + 716z^3 - 588z^4) + 275z^5 - 74z^6 + 11z^7 - z^8 \right] \log(1-z) + \frac{2}{3} n_f \frac{2-x}{x} \left[\frac{\langle Y | \mathcal{O}_8[{}^3P_1] | Y \rangle}{m^4} \right]. \quad (\text{C12})$$

2. The NLO gluonic coefficients $C_g^{(1)}[Q]$

In this section we present the NLO QCD spectrum of the gluon arising from the color-octet components. Contributions $\sim \delta(x)$ have been neglected. The gluon energy fraction is denoted by $x = E_g/m$. For $Q = {}^1S_0^{[8]}, {}^3P_0^{[8]}, {}^3P_2^{[8]}$, we have

$$C_g^{(1)}[Q] = \frac{\alpha_s}{\pi} \Gamma_{\text{Born}}[Q \rightarrow gg] \left[\log \frac{4m^2}{\mu_F^2} \mathcal{P}_{gg}(x) + 2 \log x \mathcal{P}_{gg}(x) + \left(\frac{\log(1-x)}{1-x} \right)_+ (1-x) \mathcal{P}_{gg}(x) + \left(\frac{1}{1-x} \right)_+ f[Q](x) + \left(B[Q] + 4b_0 \log \frac{\mu_R}{2m} \right) \delta(1-x) \right], \quad (\text{C13})$$

where

$$B[{}^1S_0^{[8]}] = C_F \left(-10 + \frac{\pi^2}{2} \right) + C_A \left(\frac{139}{18} - \frac{1}{12} \pi^2 \right) - \frac{10}{9} n_f T_F, \quad (\text{C14})$$

$$B[{}^3P_0^{[8]}] = C_F \left(-\frac{14}{3} + \frac{\pi^2}{2} \right) + C_A \left(\frac{235}{54} + \frac{70}{27} \log 2 - \frac{1}{12} \pi^2 \right) - \frac{10}{9} n_f T_F, \quad (\text{C15})$$

$$B[{}^3P_2^{[8]}] = -8C_F + C_A \left(5 + \frac{14}{9} \log 2 - \frac{1}{6} \pi^2 \right) - \frac{8}{45} n_f T_F, \quad (\text{C16})$$

and furthermore

$$\begin{aligned} f_g[{}^1S_0^{[8]}](x) &= \frac{C_A}{6(-2+x)^2 x} (-120 + 336x - 494x^2 + 410x^3 - 215x^4 + 72x^5 - 12x^6) \\ &\quad + \frac{2C_A(-1+x)}{(2-x)^3 x^2} (16 - 40x + 50x^2 - 26x^3 - 8x^4 + 16x^5 - 7x^6 + x^7) \log(1-x) + n_f T_F \frac{2}{3} x, \end{aligned} \quad (\text{C17})$$

$$\begin{aligned} f_g[{}^3P_0^{[8]}](x) &= \frac{C_A}{54(-2+x)^4 x^3} (-1536 + 5376x - 9632x^2 + 10016x^3 - 9288x^4 + 12976x^5 - 16906x^6 + 13918x^7 - 6623x^8) \\ &\quad + 1664x^9 - 172x^{10} + \frac{2C_A(-1+x)}{9(2-x)^5 x^4} (256 - 896x + 1504x^2 - 1008x^3 - 516x^4 + 1792x^5 - 2276x^6 + 2011x^7) \\ &\quad - 1220x^8 + 464x^9 - 99x^{10} + 9x^{11} \log(1-x) + n_f T_F \frac{2(2+x)^2}{27x}, \end{aligned} \quad (\text{C18})$$

$$\begin{aligned} f_g[{}^3P_2^{[8]}](x) &= \frac{C_A}{36(-2+x)^4 x^3} (-384 + 3072x - 12704x^2 + 25376x^3 - 30738x^4 + 26998x^5 - 19231x^6 + 10924x^7 - 4373x^8) \\ &\quad + 1028x^9 - 106x^{10} + \frac{C_A(-1+x)}{3(2-x)^5 x^4} (64 - 512x + 2032x^2 - 3840x^3 + 3747x^4 - 1577x^5 - 515x^6 + 1162x^7 - 800x^8) \\ &\quad + 308x^9 - 66x^{10} + 6x^{11} \log(1-x) + n_f T_F \frac{1}{9x} (10 - 5x + x^2). \end{aligned} \quad (\text{C19})$$

For the ${}^3S_1^{[8]}$ component we obtain

$$\begin{aligned} C_g^{(1)}[{}^3S_1^{[8]}] &= \frac{\alpha_s^3}{18} \left[\frac{1}{(-2+x)^2 x} (1168 - 3264x + 3740x^2 - 2200x^3 + 693x^4 - 108x^5) \right. \\ &\quad \left. + \frac{4(-1+x)}{(2-x)^3 x^2} (584 - 1632x + 1904x^4 - 1134x^3 + 324x^4 - 27x^5) \log(1-x) \right] \frac{\langle Y | \mathcal{O}_8[{}^3S_1] | Y \rangle}{m^2} \\ &\quad + n_f \Gamma_{\text{Born}}({}^3S_1^{[8]} \rightarrow q\bar{q}) \frac{\alpha_s}{\pi} \left[\frac{-3 + 3x - x^2}{x} + \left(\log \frac{4m^2}{\mu_F^2} + \log(1-x) + 2 \log x \right) P_{gq}(x) \right]. \end{aligned} \quad (\text{C20})$$

Finally for ${}^3P_1^{[8]}$,

$$\begin{aligned} C_g^{(1)}[{}^3P_1^{[8]}] &= \frac{5\alpha_s^3}{18} \left[\frac{1}{(-2+x)^4 x^3} (384 + 384x - 4192x^2 + 7552x^3 - 6446x^4 + 2876x^5) \right. \\ &\quad \left. - 485x^6 - 141x^7 + 82x^8 - 10x^9 \right] + \frac{12}{(-2+x)^5 x^4} (-1+x)(64 + 64x - 688x^2 + 1280x^3) \\ &\quad - 1181x^4 + 626x^5 - 195x^6 + 36x^7 - 4x^8 \log(1-x) + \frac{2}{3} n_f \frac{2-x}{x} \left] \frac{\langle Y | \mathcal{O}_8[{}^3P_1] | Y \rangle}{m^4}. \end{aligned} \quad (\text{C21})$$

3. The NLO quark coefficients $C_q^{(1)}[Q]$

We report in this section the quark energy spectrum in $Q \rightarrow q\bar{q}g$ decays. The adimensional energy of the quark E_q/m is denoted by x :

$$C_q^{(1)}[{}^1S_0^{[8]}] = \frac{\alpha_s}{\pi} \Gamma_{\text{Bom}}[{}^1S_0^{[8]} \rightarrow gg] \left[\mathcal{P}_{qg}(x) \log \frac{4m^2}{\mu_F^2} + 2x(1-x)T_F + \mathcal{P}_{qg}(x) \log[x^2(1-x)] + f[{}^1S_0^{[8]}](x) \right], \quad (\text{C22})$$

where

$$f_q[{}^1S_0^{[8]}](x) = x(1-x)[1 + \log(1-x)]. \quad (\text{C23})$$

We have

$$C_q^{(1)}[{}^3S_1^{[8]}] = \Gamma_{\text{Bom}}[{}^3S_1^{[8]} \rightarrow q\bar{q}] \frac{\alpha_s}{\pi} \left[\frac{1}{2} \mathcal{P}_{qq}(x) \log \frac{4m^2}{\mu_F^2} + C_F \frac{1+x^2}{(1-x)_+} \log x + \frac{C_F}{2} (1-x) + \frac{1}{2} (1-x) \left(\frac{\log(1-x)}{1-x} \right)_+ \mathcal{P}_{qq}(x) \right. \\ \left. + \left(\frac{1}{1-x} \right)_+ f_q[{}^3S_1^{[8]}](x) + A[{}^3S_1^{[8]}] \delta(1-x) \right], \quad (\text{C24})$$

where

$$A[{}^3S_1^{[8]}] = C_F \left(-\frac{25}{4} + \frac{\pi^2}{3} \right) + C_A \left(\frac{50}{9} + \frac{2}{3} \log 2 - \frac{\pi^2}{4} \right) - \frac{10}{9} n_f T_F + 2 \log \frac{\mu_R}{2m}, \quad (\text{C25})$$

and

$$f_q[{}^3S_1^{[8]}](x) = C_F \frac{x}{4} (-4+x) - C_A \frac{x}{2} (5-5x+2x^2) + C_A (1-x) (-2+x) \log(1-x), \quad (\text{C26})$$

$$C_q^{(1)}[{}^3P_J^{[8]}] = B_F \alpha_s^3 \delta(1-x) \left[-\frac{8}{9} \log \frac{\mu_\Lambda}{2m} + a_J \right] \frac{\langle Y | \mathcal{O}_8[{}^3P_J] | Y \rangle}{m^4} + \frac{\alpha_s}{\pi} \Gamma_{\text{Bom}}[{}^3P_J^{[8]} \rightarrow gg] \\ \times \left[2x(1-x)T_F + \log[x^2(1-x)] \mathcal{P}_{qg}(x) + \left(\frac{1}{1-x} \right)_+ f_q^{(J)}(x) + \mathcal{P}_{qg}(x) \log \frac{4m^2}{\mu_F^2} \right], \quad [J=0,2]. \quad (\text{C27})$$

We also have

$$C_q^{(1)}[{}^3P_1^{[8]}] = B_F \alpha_s^3 \delta(1-x) \left[-\frac{8}{9} \log \frac{\mu_\Lambda}{2m} + a_1 \right] \frac{\langle Y | \mathcal{O}_8[{}^3P_1] | Y \rangle}{m^4} + \alpha_s^3 B_F \left(\frac{1}{1-x} \right)_+ f_q^{(1)}(x) \frac{\langle Y | \mathcal{O}_8[{}^3P_1] | Y \rangle}{m^4}, \quad (\text{C28})$$

where

$$a_0 = \frac{2}{9}, \quad a_1 = \frac{1}{9}, \quad a_2 = \frac{7}{45}, \quad (\text{C29})$$

and finally

$$f_q^{(0)}(x) = \frac{1}{27} [x(33-72x+43x^2) - 3(1-x)(4-9x+9x^2) \log(1-x)], \quad (\text{C30})$$

$$f_q^{(1)}(x) = \frac{2}{9} [x(3+6x-5x^2) + 3(1-x) \log(1-x)], \quad (\text{C31})$$

$$f_q^{(2)}(x) = \frac{1}{36} [x(57-90x+53x^2) - 3(1-x)(5-12x+12x^2) \log(1-x)]. \quad (\text{C32})$$

- [1] CLEO Collaboration, B. Nemati *et al.*, Phys. Rev. D **55**, 5273 (1997); ARGUS Collaboration, H. Albrecht *et al.*, Phys. Lett. B **199**, 291 (1987); CLEO Collaboration, S. E. Csorna *et al.*, Phys. Rev. Lett. **56**, 1222 (1986); CUSB Collaboration, R. D. Schamberger *et al.*, Phys. Lett. **138B**, 225 (1984).
- [2] S. J. Brodsky, T. A. DeGrand, R. R. Horgan, and D. G. Coyne, Phys. Lett. **73B**, 203 (1978).
- [3] R. D. Field, Phys. Lett. **133B**, 248 (1983).
- [4] G. T. Bodwin, E. Braaten, and G. P. Lepage, Phys. Rev. D **51**, 1125 (1995); **55**, 5853(E) (1997).
- [5] S. Catani and F. Hautmann, Nucl. Phys. B (Proc. Suppl.) **54A**, 247 (1997); F. Hautmann, hep-ph/9708496.
- [6] J. F. Owens, Rev. Mod. Phys. **59**, 465 (1987).
- [7] I. Z. Rothstein and M. B. Wise, Phys. Lett. B **402**, 346 (1997); T. Mannel and S. Wolf, hep-ph/9701324.
- [8] P. Aurenche, P. Chiappetta, M. Fontannaz, J. P. Guillet, and E. Pilon, Nucl. Phys. **B399**, 34 (1993); L. Bourhis, M. Fontannaz, and J. Ph. Guillet, Eur. Phys. J. C **2**, 529 (1998).
- [9] M. Glück, E. Reya, and A. Vogt, Phys. Rev. D **48**, 116 (1993).
- [10] B. Mele, P. Nason, and G. Ridolfi, Nucl. Phys. **B357**, 409 (1991); M. L. Mangano, P. Nason, and G. Ridolfi, *ibid.* **B373**, 295 (1992).
- [11] A. Petrelli, M. Cacciari, M. Greco, F. Maltoni, and M. L. Mangano, Nucl. Phys. **B514**, 245 (1998).
- [12] F. Maltoni, M. L. Mangano, and A. Petrelli, Nucl. Phys. **B519**, 361 (1998).
- [13] P. Cho and A. K. Leibovich, Phys. Rev. D **53**, 150 (1996); **53**, 6203 (1996).
- [14] M. Cacciari and M. Krämer, Phys. Rev. Lett. **76**, 4128 (1996).
- [15] M. Gremm and A. Kapustin, Phys. Lett. B **407**, 323 (1997).
- [16] R. Barbieri, R. Gatto, R. Kögerler, and Z. Kunszt, Phys. Lett. **57B**, 455 (1975).
- [17] P. B. Mackenzie and G. P. Lepage, Phys. Rev. Lett. **47**, 1244 (1981).
- [18] W.-Y. Keung and I. J. Muzinich, Phys. Rev. D **27**, 1518 (1983); P. Labelle, G. P. Lepage, and U. Magnea, Phys. Rev. Lett. **72**, 2006 (1994); G. Schuler, Report No. CERN-TH.7170, 1994, hep-ph/9403387.
- [19] Particle Data Group, R. M. Barnett *et al.*, Phys. Rev. D **54**, 1 (1996).
- [20] P. M. Stevenson, Phys. Lett. **100B**, 61 (1981); Phys. Rev. D **23**, 2916 (1981).
- [21] M. Beneke, A. Signer, and V. A. Smirnov, Phys. Rev. Lett. **80**, 2535 (1998).
- [22] M. Beneke, I. Z. Rothstein, and M. B. Wise, Phys. Lett. B **408**, 373 (1997).
- [23] M. Beneke, M. Krämer, and M. Vanttinen, Phys. Rev. D **57**, 4258 (1998).